Chemical Science

ROYAL SOCIETY OF CHEMISTRY

EDGE ARTICLE

View Article Online
View Journal | View Issue

Cite this: *Chem. Sci.*, 2023, **14**, 849

All publication charges for this article have been paid for by the Royal Society of Chemistry

Multifaceted behavior of a doubly reduced arylborane in B–H-bond activation and hydroboration catalysis†

Sven E. Prey,‡[a] Christoph Herok,‡[b] Felipe Fantuzzi,[bc] Michael Bolte,[a] Hans-Wolfram Lerner,[a] Bernd Engels*[b] and Matthias Wagner*[a]

Alkali-metal salts of 9,10-dimethyl-9,10-dihydro-9,10-diboraanthrancene (M_2[DBA-Me_2]; M^+ = Li^+, Na^+, K^+) activate the H–B bond of pinacolborane (HBpin) in THF already at room temperature. For M^+ = Na^+, K^+, the addition products M_2[**4**] are formed, which contain one new H–B and one new B–Bpin bond; for M^+ = Li^+, the H^- ion is instantaneously transferred from the DBA-Me_2 unit to another equivalent of HBpin to afford Li[**5**]. Although Li[**5**] might commonly be considered a [Bpin]$^-$ adduct of neutral DBA-Me_2, it donates a [Bpin]$^+$ cation to Li[$SiPh_3$], generating the silyl borane Ph_3Si–Bpin; Li_2[DBA-Me_2] with an aromatic central B_2C_4 ring acts as the leaving group. Furthermore, Li_2[DBA-Me_2] catalyzes the hydroboration of various unsaturated substrates with HBpin in THF. Quantum-chemical calculations complemented by *in situ* NMR spectroscopy revealed two different mechanistic scenarios that are governed by the steric demand of the substrate used: in the case of the bulky Ph(H)C=N*t*Bu, the reaction requires elevated temperatures of 100 °C, starts with H–Bpin activation which subsequently generates Li[BH_4], so that the mechanism eventually turns into "hidden borohydride catalysis". Ph(H)C=NPh, Ph_2C=O, Ph_2C=CH_2, and *i*PrN=C=N*i*Pr undergo hydroboration already at room temperature. Here, the active hydroboration catalyst is the [4 + 2] cycloadduct between the respective substrate and Li_2[DBA-Me_2]: in the key step, attack of HBpin on the bridging unit opens the bicyclo[2.2.2]octadiene scaffold and gives the activated HBpin adduct of the Lewis-basic moiety that was previously coordinated to the DBA-B atom.

Received 5th October 2022
Accepted 2nd December 2022

DOI: 10.1039/d2sc05518j

rsc.li/chemical-science

Introduction

The activation of chemical bonds by main-group compounds is not only conceptually appealing, but also holds great application potential. A prominent class of p-block catalysts is that of Frustrated Lewis Pairs (FLPs), which contain suitable combinations of sterically encumbered Lewis acids (LA) and bases (LB). Together, these functional units contribute the vacant orbital and electron lone pair which, in classical catalysis, are provided by one single transition metal center with partially filled d orbitals.[1,2] More recently, alternative systems based on doubly boron-doped (hetero)arenes have been reported.[3,4] Common to all of them is a central six-membered ring featuring an aromatic π-electron system and two mutually cooperating B atoms integrated therein at opposite positions. As an example, Kinjo *et al.* disclosed that the 1,3,2,5-diazadiborinine **A** (Fig. 1) adds the single bond of H_3C–OSO_2CF_3, the double bonds of alkenes and carbonyls, as well as the triple bonds of alkynes across its B sites. As mode of action, Kinjo postulated that **A** has a B(I)/B(III) mixed-valence character,[5–7] which would render it formally analogous to an LB/LA FLP. A related 1,4,2,5-diazadiborinine activates H–H, B–H, Si–H, and P–H bonds. Here, it was proposed that the two chemically equivalent B atoms "act as both nucleophilic and electrophilic centers, demonstrating ambiphilic nature".[8,9] Catalytic cycles based on these diazadiborinines have not yet been described, with one notable exception: *in situ*-generated [4 + 2] cycloadducts of **A** and Ph(Me)C=O or H_2C=CH_2 act as "electrostatic catalysts" to promote hydroboration of carbonyl compounds with pinacolborane (HBpin; see Fig. 3 below).[7]

Wagner and coworkers have introduced 9,10-dihydro-9,10-diboraanthracene (DBA) dianions [DBA-R_2]$^{2-}$ into catalysis (Fig. 1; R = H, Me). These species have indistinguishable, sterically accessible B atoms along with high-lying HOMO-

[a]*Institut für Anorganische und Analytische Chemie, Goethe-Universität Frankfurt, Frankfurt am Main D-60438, Germany. E-mail: matthias.wagner@chemie.uni-frankfurt.de*

[b]*Institut für Physikalische und Theoretische Chemie, Julius-Maximilians-Universität Würzburg, Würzburg D-97074, Germany. E-mail: bernd.engels@uni-wuerzburg.de*

[c]*School of Chemistry and Forensic Science, University of Kent, Canterbury CT2 7NH, UK*

† Electronic supplementary information (ESI) available: Synthetic procedures, NMR spectra, X-ray crystallographic data and computational details. CCDC 2207512–2207520. For ESI and crystallographic data in CIF or other electronic format see DOI: https://doi.org/10.1039/d2sc05518j

‡ These authors contributed equally.

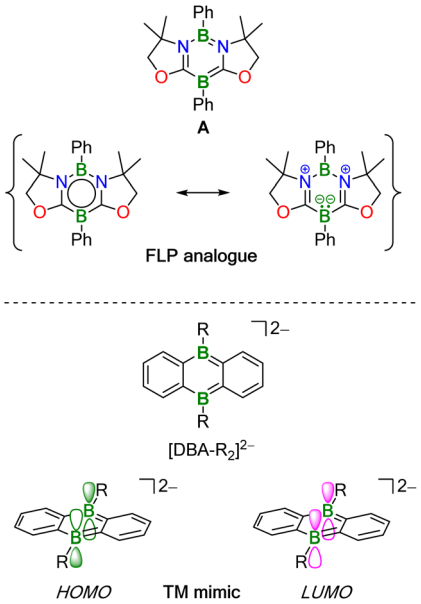

Fig. 1 (Top) 1,3,2,5-Diazadiborinine **A** can be regarded as B(I)/B(III) mixed-valence system, which activates substrate molecules in a similar manner to LB/LA-FLPs. (Bottom) The frontier orbital symmetries of the 9,10-dihydro-9,10-diboraanthracene (DBA) dianion $[DBA\text{-}R_2]^{2-}$ allow concerted transition metal-like (TM-like) reactions.

energy levels and are therefore particularly reactive. Apart from reacting with H–H and C–H bonds, $[DBA\text{-}R_2]^{2-}$ dianions undergo facile [4 + 2] cycloaddition with various unsaturated organic molecules.[10–14]

The HOMO and LUMO of $[DBA\text{-}R_2]^{2-}$ have the same local symmetries about the B atoms as, respectively, the LUMO and HOMO of H_2, and quantum-chemical calculations suggest a concerted, transition metal-like (TM-like) bond-cleavage pathway (Fig. 1).[11] H_2 activation by $[DBA\text{-}R_2]^{2-}$ is at the core of two recently developed catalytic hydrogenation- and H^--transfer cycles.[13] In addition, it has been shown that $[DBA\text{-}R_2]^{2-}$ can catalyze the disproportionation of CO_2 to CO and $[CO_3]^{2-}$.[12,15]

In a joint experimental and theoretical effort, we are herein unveiling the capacity of the $[DBA\text{-}R_2]^{2-}$ platform to activate B–H bonds and catalyze hydroborations. Besides our system, there are also numerous FLPs that catalyze hydroborations. Various modes of action have been discussed.[16] The hydroboration reaction is therefore an ideal tool to put into context the behavior of $[DBA\text{-}R_2]^{2-}$ dianions with those of other main group catalysts and to learn more about the subtleties of subvalent boron species.

Three key results are disclosed: (i) HBpin activation by $[DBA\text{-}R_2]^{2-}$ is a means of forming new B–B bonds. (ii) Depending on the steric bulk of the substrate, the hydroboration mechanism differs between "hidden borohydride catalysis"[17] and actual DBA-driven catalysis. (iii) To gain accurate theoretical insights into the mechanisms, one must explicitly include the counter cations and their coordinating solvent molecules in the calculations, since simple continuum approaches are too imprecise.

Results and discussion

All reactions were performed in (deuterated) tetrahydrofuran (THF, THF-d_8).

Activation of HBpin by $M_2[DBA\text{-}R_2]$

Pinacolborane (HBpin) was selected as the hydroboration reagent for the following reasons: (i) in contrast to, *e.g.*, B_2H_6 or $(9\text{-BBN})_2$ (BBN = 9-borabicyclo[3.3.1]nonane), HBpin is strictly monomeric[18] and does not form solvent adducts in THF, which facilitates the theoretical assessment of its reactivity. (ii) The alkyl boronic ester products (R′–Bpin) are comparatively stable to air and moisture, easy to purify, and have a wide range of applications.[19] The aforementioned assets are the result of pronounced O=B π donation, decreasing the electrophilicity of the B atom. On the other hand, less Lewis-acidic boranes are less prone to spontaneous addition to unsaturated substrates, so that a catalyst is often required. Thus, hydroboration reactions with HBpin provide the ideal setting to further explore the scope of $M_2[DBA\text{-}R_2]$-mediated reactions.

Our investigations into the activation of HBpin by $M_2[DBA\text{-}R_2]$ were carried out with $M^+ = Li^+$–K^+ as counter cations and R = H, Me as B-bonded substituents (Li_2[**1**]–K_2[**1**], Li_2[**2**]–K_2[**2**]; Scheme 1). In all cases, the reaction with HBpin was already instantaneous at room temperature, as judged by the rapid fading of the intensely colored $M_2[DBA\text{-}R_2]$ solutions after addition of the borane ($M^+ = Li^+$: red; $M^+ = Na^+$, K^+: green). According to *in situ* NMR spectroscopy, 1 equiv. of HBpin was sufficient to quantitatively convert Na_2[**1**], K_2[**1**], and K_2[**2**] to

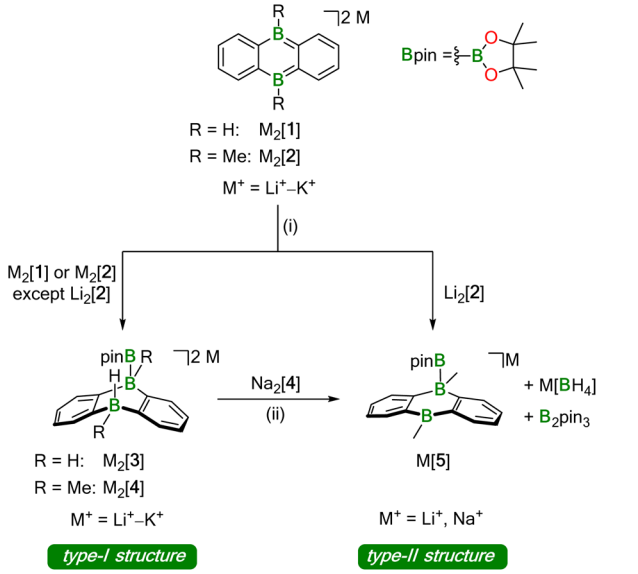

Scheme 1 Addition of pinacolborane (HBpin) across the two B atoms of 9,10-dihydro-9,10-diboraanthracene (DBA) dianions to form B–B bonds. Depending on the nature of the counter cations, the dianionic type-I structures compete with monoanionic type-II structures, which are formed by transfer of the H^- ligand onto a second equivalent of HBpin. (i) 1–5 equiv. HBpin (see ESI†), THF-d_8, room temperature; (ii) prolonged storage in 1,2-dimethoxyethane (DME) during crystallization experiments.

Na_2[**3**], K_2[**3**], and K_2[**4**], respectively, featuring newly formed B–H and B–Bpin bonds together with two tetracoordinate B centers on their DBA cores (type-I structures; Scheme 1). In contrast, equimolar mixtures of Li_2[**1**] or Na_2[**2**] with HBpin contained Li_2[**3**] or Na_2[**4**] and significant amounts of still unconsumed starting materials. Full conversion of the DBA-dianion salts to the corresponding type-I addition products required the use of excess HBpin. These $[DBA\text{-}R_2]^{2-}$-reactivity trends are the same as those previously reported for H_2 activation:[13] (i) M^+ ions with larger charge-radius ratio have a higher tendency to form contact–ion pairs with $[DBA\text{-}R_2]^{2-}$ in solution, which leads to the reactivity order $Li_2[DBA\text{-}R_2] < Na_2[DBA\text{-}R_2] < K_2[DBA\text{-}R_2]$.[11] (ii) Smaller B-bonded substituents R impede substrate access to $[DBA\text{-}R_2]^{2-}$ less than bulkier groups, resulting in the reactivity order $[\mathbf{2}]^{2-} < [\mathbf{1}]^{2-}$.

The accordingly least reactive Li_2[**2**] is indeed a peculiarity, since a type-I product (putative Li_2[**4**]) could not even be detected as an intermediate. Rather, the monoanion salt Li[**5**] was formed without H^- ligand at the DBA moiety (type-II structure; Scheme 1). Again, an excess of HBpin was necessary to enforce quantitative transformation of Li_2[**2**] to Li[**5**], which is accompanied by a formal release of LiH. According to quantum-chemical calculations, this would be an energetically unfavorable process[20,21] and it is, therefore, reasonable to assume that excess HBpin acts as H^- scavenger. The NMR-spectroscopically observed formation of $[BH_4]^-$ and B_2pin_3 (ref. 22) supports this assumption, since H^- is known to induce a corresponding decay of HBpin.[17] In summary, we propose that Li_2[**2**] and HBpin are in a dynamic addition–elimination equilibrium, which is shifted towards Li[**5**] formation by H^- transfer to HBpin and the subsequent irreversible decomposition of the resulting $[H_2Bpin]^-$ adduct. Consistent with this view, addition of LiH to a THF-d_8 solution of Li[**5**] leads back to Li_2[**2**] and HBpin (NMR-spectroscopic control).

The characteristic NMR data of type-I/II structures are exemplarily discussed with reference to the Na_2[**4**]/Li[**5**] couple. The ^{11}B NMR spectrum of Na_2[**4**] contains three signals. Two of them appear in the chemical shift range of tetracoordinate B nuclei [−22.0 ppm (*B*Bpin), −17.4 ppm (d, $^1J_{BH}$ = 68 Hz, BH)] and the third is characteristic of a tricoordinate B center [42.6 ppm (broad, Bpin)].[23] The $\delta(^{11}B)$ values of Li[**5**] prove the presence of one tetra- and two tricoordinate B atoms [−19.7 ppm (*B*Bpin), 41.6 ppm (Bpin), 61.8 ppm (BC_3)]. Accordingly, only the $^1H\{^{11}B\}$ NMR spectrum of Na_2[**4**] shows the signal of a B-bonded H atom (2.14 ppm). The ^{1}H integral values in the spectra of both Na_2[**4**] and Li[**5**] are consistent with the presence of one Bpin substituent in each of these molecules. In line with the proposed average C_s symmetry of Na_2[**4**] and Li[**5**] in solution, their $^{13}C\{^1H\}$ NMR spectra exhibit only six resonances in the aromatic region. Single crystals of the type-II compound $[Li(thf)_2]$[**5**] were grown by gas-phase diffusion of *n*-hexane into a C_6H_6 solution of thf-solvated Li[**5**] (Fig. 2). Attempts at the crystallization also of type-I compounds gave specimens suitable for X-ray diffraction only from 1,2-dimethoxyethane (DME) solutions of thf-solvated Na_2[**4**] (room temperature, 1–2 d). Since X-ray analysis revealed that the crystals consisted of $[Na(thf)_2]$[**5**] as opposed to Na_2[**4**] (Fig. 2), it appears that Na_2[**4**] is also susceptible to formal NaH elimination (triggered by residual HBpin under the crystallization conditions). The DBA moiety of $[Na(thf)_2]$[**5**] has one sp^3-hybridized [B(1)] and one sp^2-hybridized B atom [B(2); $\sum(\measuredangle CBC) = 360.0°$]. At B(1), the Bpin substituent is attached in an axial position and with a bond length of B(1)–B(3) = 1.731(9) Å.[24] The $[Na(thf)_2]^+$ cation is coordinated by an O atom belonging to Bpin and by the centroid of a phenylene ring, creating a contact–ion pair. The solid-state structure of $[Li(thf)_2]$[**5**] does not merit further discussion, given that it differs from that of $[Na(thf)_2]$[**5**] mainly in details of cation–anion association.[20]

Reactivities of $M_2[DBA\text{-}R_2]$/HBpin addition products

Hydridoborate ions $[R_3B\text{–}H]^-$ and negatively charged adducts $[R_3B\text{–}Bpin]^-$ are widely used sources of H^- and $[Bpin]^-$ nucleophiles, respectively.[25,26] Type-I compounds such as Na_2[**4**] provide both functionalities in the same molecule, which raises the question of whether H^- or $[Bpin]^-$ are preferentially transferred to, *e.g.*, chlorosilanes as archetypal electrophiles. Treatment of freshly prepared Na_2[**4**] with 1 equiv. of Et_3SiCl resulted in selective H^- abstraction to form Na[**5**] and Et_3SiH, showing that H^- wins the competition [*cf.* abstraction of MH by HBpin during the formation of M[**5**] ($M^+ = Li^+$, Na^+)]. What about the possibility of $[Bpin]^-$ transfer in the absence of a competing H^- ion? We have found that Li[**5**] is inert to Et_3SiCl, Et_3SiBr, and MeI at room temperature for several days and therefore does not

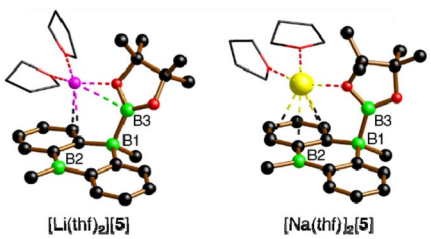

Fig. 2 X-ray-crystallographically derived solid-state structures of the solvates $[Li(thf)_2]$[**5**] and $[Na(thf)_2]$[**5**], featuring one B–Bpin bond. C-bonded H atoms are omitted for clarity; the thf ligands are simplified as wireframes; Li: pink, B: green, C: black, O: red, Na: yellow spheres.

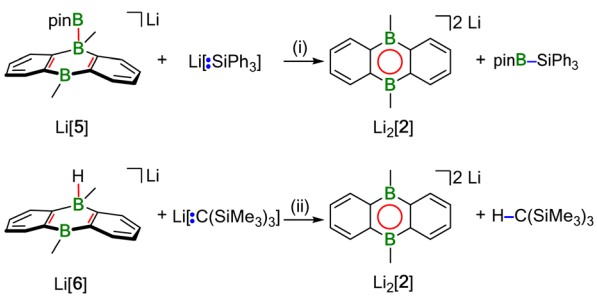

Scheme 2 Reactions of Li[**5**] and Li[**6**] with an Si-centered nucleophile and a C-centered Brønsted base to demonstrate transfer of $[Bpin]^+$ and H^+ along with the suitability of $[\mathbf{2}]^{2-}$ as leaving group. (i) THF-d_8, room temperature, overnight; (ii) THF-d_8, 115 °C, 35 h.

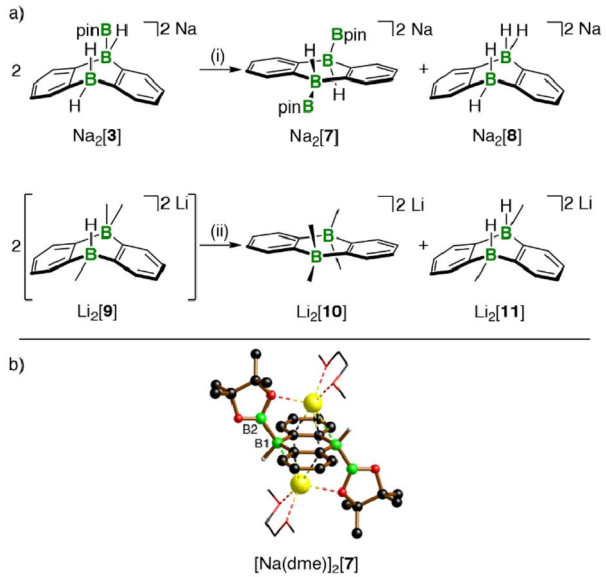

Scheme 3 (a) Substituent-redistribution reaction at Na_2[**3**] producing Na_2[**7**] with two B–Bpin bonds. Substituent-redistribution reaction at Li_2[**9**] leading to the pair of more symmetric compounds Li_2[**10**]/Li_2[**11**]. (b) X-ray-crystallographically derived solid-state structure of the solvate [Na(dme)]$_2$[**7**], featuring two B–Bpin bonds. C-bonded H atoms are omitted for clarity; the dme ligands are shown as wireframes; B: green, C: black, O: red, Na: yellow spheres. (i) DME, room temperature, prolonged storage during crystallization experiments; (ii) THF-d_8, room temperature.

appear to be a [Bpin]$^-$ donor. To probe if a polarity-inverted reactivity is present, Li[**5**] was next combined with the silanide salt Li[$SiPh_3$], which indeed gave pinB–$SiPh_3$ (ref. 27) in a clean reaction.[28] Here, the highly delocalized byproduct [**2**]$^{2-}$ turns out to be a good enough leaving group to promote the transfer of a [Bpin]$^+$ electrophile (Scheme 2). To confirm this remarkable result further, we also prepared the formal hydridoborate anion Li[**6**] through H$^-$-adduct formation between the Lewis acid **2** and the H$^-$ source LiH and then removed H$^+$ by deprotonation of Li[**6**] with Li[$C(SiMe_3)_3$][29] (Scheme 2).[20] Again, [**2**]$^{2-}$ is liberated, accompanied by the formation of $HC(SiMe_3)_3$, which renders Li[**6**] a model system of Li[**5**] in which all reactive parts are stripped down to their absolute essence.[30]

The reactions between M_2[**1**]/M_2[**2**] and HBpin described up to this point are not only relevant for H–B-bond activation, but also represent B–B-bond formation reactions off the beaten track. The latter aspect gains additional weight because Na_2[**3**] (one B–B bond) is prone to H$^-$/[Bpin]$^-$ scrambling, thereby generating a DBA with two B–B bonds: When a DME solution of Na_2[**3**] was stored at room temperature, [Na(dme)]$_2$[**7**] precipitated in single-crystalline form (Scheme 3).

The dianion [**7**]$^{2-}$ can be regarded as Lewis pair {**1**·2[Bpin]$^-$}; the necessary byproduct Na_2[**8**][11,13] remained in the mother liquor and was detected by NMR spectroscopy after workup.

The ^{1}H, ^{11}B, and ^{13}C{^{1}H} NMR spectroscopic characterization of re-dissolved [Na(dme)]$_2$[**7**] was in line with an average C_{2v} or C_{2h} symmetry but allowed no conclusion regarding a mutual *cis* or *trans* orientation of the two Bpin ligands. The assignment of [Na(dme)]$_2$[**7**] as a C_i-symmetric *trans* complex ($\hat{=}$ C_{2h} in solution) was finally achieved by X-ray crystallography (B(1)–B(2) = 1.711(3), Scheme 3). Note that the attempted synthesis of *cis*-Na_2[**7**] from Na_2[**1**] and B_2pin_2 failed, because the two compounds do not react with each other. Also the investigation of the transformation 2 Na_2[**3**] → Na_2[**7**] + Na_2[**8**] was complemented by a model reaction, in which a Me group mimicked the Bpin group of Na_2[**3**] (Scheme 3): Addition of MeLi (1 equiv.) to Li[**6**] did not lead to an NMR-spectroscopically detectable diadduct Li_2[**9**], but rather to an equimolar mixture of the more symmetric Li_2[**10**] and Li_2[**11**][13] scrambling products,[20] the former corresponding to Na_2[**7**].

Taken together, a clear picture of the reactivity trends of the DBA substituents emerges from the model studies, which is of immediate importance with respect to the transfer of H or Bpin fragments onto substrates in the course of hydroboration reactions: a substituent R residing on the tetracoordinate B atom of a B(sp^2),B(sp^3)-DBA can be removed as an R$^+$ fragment because the formerly B–R-bonding electron pair subsequently becomes part of a Clar's sextet[31] within the central B_2C_4 ring. However, in a B(sp^3),B(sp^3)-DBA, this energetically favorable electron delocalization after R$^+$ transfer is blocked by the second tetracoordinate B atom, which is why the same R now possesses mainly R$^-$ character.

Hydroboration reactions

The substrates under investigation contained less polar (C=C) as well as more polar (C=N, C=O) double bonds and possessed different steric demands (*e.g.*, Ph(H)C=NPh < Ph(H)C=N*t*Bu). Hydroborations were regularly performed with a loading of 25 mol% Li_2[**2**] to facilitate the NMR-spectroscopic detection of reaction intermediates, side products, and byproducts; in the selected case of Ph_2C=O, it was confirmed that a Li_2[**2**] loading of 5 mol% is sufficient for full conversion of the starting materials and thus the reactions are truly catalytic in the DBA. To ensure full comparability, we always added the HBpin to a mixture of freshly prepared Li_2[**2**] and the unsaturated substrate.[32]

Two fundamentally different reaction mechanisms were found to be operative under these conditions.[33] Which of the two comes into play depends decisively on the steric requirements of the substrate. Only in the case of the bulkiest substrate, the imine Ph(H)C=N*t*Bu, does HBpin activation by Li_2[**2**] initiate the transformation; the actual catalytic cycle is a textbook example of "hidden borohydride catalysis".[17] In all other cases, [4 + 2] cycloaddition of the substrates' double bonds occurs prior to HBpin addition; subsequent hydroboration is then catalyzed by the cycloadducts.

Mechanism I: hidden borohydride catalysis. NMR spectra recorded on a freshly prepared mixture of Li_2[**2**], Ph(H)C=N*t*Bu, and HBpin showed the characteristic resonances of the above-mentioned HBpin-activation product Li[**5**], together with the signals of Li[BH_4] and B_2pin_3. The resonances of the imine were still prominently visible, and the spectrum did not indicate transformation of this starting material. The situation remained unchanged for several hours at room temperature.

Yet, heating the sample to 100 °C for 40 h led to 85% conversion of the imine, but it took another 50 h at 100 °C to drive the reaction to completion. The NMR data of the borylamine primary product agreed well with literature data;[34] after *in situ* hydrolysis, we observed the resonances of the free amine $Ph(H)_2C–N(H)tBu$.[13] We took the initial appearance of the $[BH_4]^-$ ion as a warning signal that the present case might be an example of hidden catalysis by the system $BH_3\cdot thf/[BH_4]^-$.[17] Indeed, preliminary quantum-chemical calculations indicated that such a process might be at play (see below for an in-depth theoretical treatment of the reaction mechanism). To substantiate the assumption of hidden borohydride catalysis further, we adapted a test reaction recommended by Thomas and coworkers[17] and repeated the experiment in the presence of *N*,*N*,*N*′,*N*′-tetramethylethylenediamine (TMEDA), which is supposed to act as a BH_3 scavenger. Subsequently, we detected the diagnostic signal of $(BH_3)_2\cdot tmeda$[35] and noted a significantly slower reaction. All in all, this confirmed our working hypothesis that the hydroboration of Ph(H)C=N*t*Bu by HBpin is only initiated by Li_2[**2**], but catalyzed by $BH_3\cdot thf/[BH_4]^-$.

Mechanism II: DBA-cycloadduct catalysis. Hydroborations of Ph(H)C=NPh, Ph_2C=O, and Ph_2C=CH_2 with HBpin in the presence of Li_2[**2**] proceeded quantitatively already at room temperature (Table 1). We found that the key elements of each reaction scenario are the same for all three substrates. It is therefore sufficient to discuss the experimental facts using Ph(H)C=NPh as an example. Imine Ph(H)C=NPh undergoes an instantaneous and quantitative [4 + 2] cycloaddition reaction with Li_2[**2**] to afford the dianionic bicyclo[2.2.2]octadiene derivative Li_2[**12**] (Scheme 4). As a distinct difference, the corresponding cycloaddition with the bulkier Ph(H)C=N*t*Bu is very slow at room temperature (and underlies a dynamic addition–elimination equilibrium at 100 °C).[13] Consequently, under the prevailing reaction conditions, only in the case of Ph(H)C=N*t*Bu is free Li_2[**2**] still available for initial HBpin activation, while in the other cases the actual active species must be a different one. Thus, the different steric demands of Ph(H)C=N*t*Bu and, *e.g.*, Ph(H)C=NPh lead to a bifurcation of the reaction mechanism into Mechanism I and a new Mechanism II.

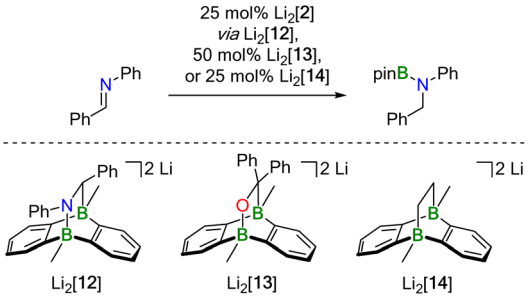

Scheme 4 Crossover experiment to demonstrate that hydroboration of Ph(H)C=NPh with HBpin can be mediated not only by Li_2[**2**] (actual catalyst: Li_2[**12**]), but also by pre-formed Li_2[**13**] or Li_2[**14**] without generating $Ph_2(H)C–OBpin$ or $H_3C–CH_2Bpin$ as crossover side product, respectively (THF-d_8, room temperature). Note that the high catalyst loadings were used for the sole purpose of being able to detect any catalyst degradation or trace formation of crossover products by NMR spectroscopy.

Probable candidate catalysts under Mechanism II would be the respective [4 + 2] cycloadducts. This assumption is supported by crossover experiments in which the hydroboration of Ph(H)C=NPh was efficiently mediated by pre-formed Li_2[**13**] or Li_2[**14**], obtained from Li_2[**2**] and Ph_2C=O or H_2C=CH_2, respectively. According to *in situ* NMR spectroscopy, the reactions furnished exclusively $Ph(H)_2C–N(Bpin)Ph$ (and no

Table 1 Hydroboration of unsaturated substrates proceeding *via* DBA-cycloadduct catalysis

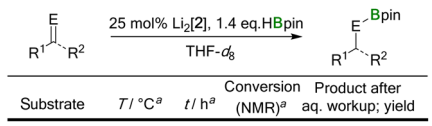

Substrate	*T* / °C[a]	*t* / h[a]	Conversion (NMR)[a]	Product after aq. workup; yield
	r. t. (100)	4 (35)	100% (29%)	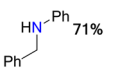 71%
	r. t. (50)	< 0.1 (3)	100% (40%)	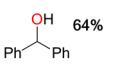 64%
	r. t. (100)	21 (18)	100% (0%)	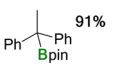 91%
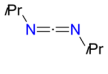	r. t. (r. t.)	< 0.1 (24)	100% (54%)	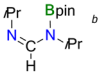 [b]

[a] Numbers in brackets refer to the blind test in the absence of Li_2[**2**]. [b] Pure samples of *i*PrN=C(H)–N(Bpin)*i*Pr were only obtained by sublimation from the reaction mixture, albeit with substantial decrease of the yield.

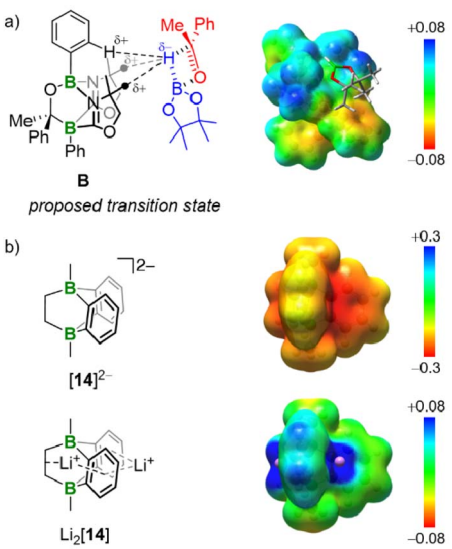

Fig. 3 Comparison of Lewis structures and computed charge densities of (a) Kinjo's bicyclic catalyst **B** and (b) compounds $[\mathbf{14}]^{2-}$ and Li_2[**14**].

$Ph_2(H)C–OBpin$ or $H_3C–CH_2Bpin$), leaving Li_2[**13**] or Li_2[**14**] intact (Scheme 4).

At first glance, the molecular scaffolds of $[\mathbf{12}]^{2-}$, $[\mathbf{13}]^{2-}$, and $[\mathbf{14}]^{2-}$ may appear similar to Kinjo's bicyclic compound **B** (Fig. 3a), which he employed as "electrostatic catalyst" for the hydroboration of various aldehydes and ketones. Here, the key to activation of the H–Bpin bond is believed to lie in electrostatic interactions between the negative partial charge on the borane's H atom and positively polarized regions in the binding pocket of **B**.[7]

However, decisive differences between Kinjo's and our catalysts should arise from (i) the presence of electronegative N and O atoms in **B**, which are (largely) absent in $[\mathbf{12}]^{2-}$, $[\mathbf{13}]^{2-}$, and $[\mathbf{14}]^{2-}$, and (ii) the fact that **B** is a neutral compound whereas our catalysts are dianion salts. A comparison of the computed charge densities of **B**, $[\mathbf{14}]^{2-}$, and Li_2[**14**] confirms this view (Fig. 3b): while positively polarized regions are indeed found in the binding pocket of **B**, they are completely missing in $[\mathbf{14}]^{2-}$. If the Li^+ counter cations are included in the charge-density calculations, positively polarized areas also emerge for Li_2[**14**] but remain largely associated with Li^+. Although the charge distribution in Li_2[**14**] does not directly correspond to the charge distribution in the binding pocket of **B**, it would nevertheless be conceivable that an interaction between the negatively polarized borane-H atom and one of the Li^+ cations could still activate the H–Bpin bond.[36] However, our calculations show that Li^+ and HBpin preferentially interact *via* an O atom (and not the H atom) of the borane (Fig. S93†).[37,38] Kinjo's mechanism is therefore not applicable to our case.

What is a plausible alternative? Although a dynamic equilibrium Li_2[**C**] ⇄ Li_2[**2**] + substrate does not exist at room temperature for the substrates Ph(H)C=NPh, Ph_2C=O, and Ph_2C=CH_2, it is conceivable that HBpin attack induces the reversible cleavage of one E–B(bridgehead) bond of Li_2[**C**] (Scheme 5; E = CH_2, NPh, O). In other words, there may be a competition between the B atoms of DBA and HBpin for the same E^- donor. Precedence exists in the form of the acetone/Na_2[**2**] cycloadduct Na_2[**15**], which straightforwardly inserts CO_2 into its O–B bond to afford Na_2[**16**] (Scheme 5).[12] In the putative

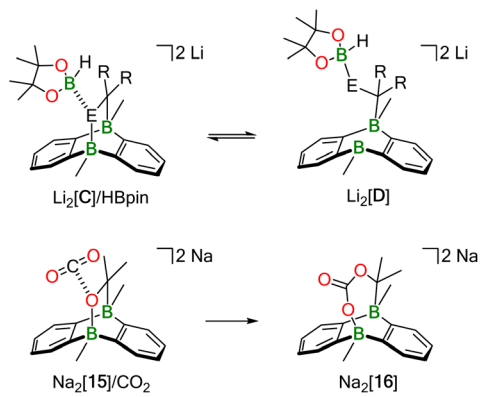

Scheme 5 Conceptual relationship between H–Bpin activation by Li_2[**C**] and CO_2 activation by Na_2[**15**] ($R_2C–E$ = $H_2C–CH_2$, $Ph_2C–CH_2$, Ph(H)C–NPh, $Ph_2C–O$).

negatively charged adduct $[\mathbf{D}]^{2-}$, the electronic situation at the H–B bond should be comparable to the case of, *e.g.*, $[BH_4]^-$. Thus, hydride transfer from $[\mathbf{D}]^{2-}$ to the unsaturated substrate, followed by "$[Bpin]^+$" transfer, would yield the respective hydroboration product and regenerate the catalyst Li_2[**C**]. Like Mechanism I, the essence of Mechanism II has also been confirmed by quantum-chemical calculations (*vide infra*).

Switch between Mechanisms I and II in the double hydroboration of *i*PrN=C=N*i*Pr. The carbodiimide *i*PrN=C=N*i*Pr has two C=N bonds and can therefore be singly or doubly hydroborated. So far, no catalyst has been described to promote both reaction scenarios.[39–43] We now report that Li_2[**2**] can catalyze the monohydroboration of *i*PrN=C=N*i*Pr to give *i*PrN=C(H)–N(Bpin)*i*Pr (room temperature, instantaneous). The reaction is selective even in the presence of 2.4 equiv. of HBpin and proceeds *via* Mechanism II (the moderate steric bulk of the heterocumulene allows formation of its [4 + 2] cycloadduct, which has been fully characterized).[20] Upon heating the sample to 100 °C (23 h), a second hydroboration furnishes *i*Pr(pinB)N–CH_2–N(Bpin)*i*Pr. Due to the larger steric bulk of *i*PrN=C(H)–N(Bpin)*i*Pr compared to *i*PrN=C=N*i*Pr, Mechanism I is operative in the second step (the $[BH_4]^-$ ion was detected by *in situ* NMR spectroscopy).

Quantum chemical calculations

Technical details. Geometry optimizations and Hessian calculations were performed at the ωB97XD/6-31+G(d,p)[44–46] level of theory including implicit solvation by the solvent model based on density (SMD).[47] Our analysis showed that explicit treatment of solvent molecules is crucial to obtain a correct description of entropy contributions along the reaction path as well as reliable kinetic barrier heights. Therefore, the optimal solvent coordination number for each intermediate was determined by free energy calculations (for details, see Fig. S94†). Unless otherwise denoted, optimized geometries were confirmed to be the desired minimum-energy structures or transition states by vibrational frequency analysis. Single-point calculations were performed at the SMD/ωB97XD/6-311++G(d,p) level (solvent: THF; ε = 7.4257). All free-energy values were calculated for the corresponding experimental temperature and included a concentration correction[48,49] that accounts for the change in standard states going from gas phase to condensed phase. All calculations were performed in Gaussian 16, Revision A.03.[50]

Computational characterization of hydroboration Mechanism I. Since well-explored hidden borohydride catalysis plays a prominent role in Mechanism I while our primary interest lies in the characterization of DBA-catalyzed hydroboration reactions, we limited the investigation of Mechanism I to key intermediates and did not calculate kinetic barriers. In order to determine the reaction mechanism, a variety of possible reaction paths was considered (at the experimental temperature of 100 °C).

Since our above-mentioned experimental results exclude direct H^- transfer from Li_2[**4**] to Ph(H)C=N*t*Bu, a corresponding reaction mechanism was not considered theoretically.

Rather, inspired by experiments of Clark and coworkers,[51] we presumed that HBpin would be able to take up the H^- ion provided by Li_2[**4**], forming Li[H_2Bpin], analogous to Clark's reactive species [*t*BuO(H)Bpin]$^-$. HBpin could thereby act as H^- shuttle to Ph(H)C═NtBu. Indeed, this approach led to an overall exergonic reaction (−24 kcal mol^{-1}) with the free energy of the highest-lying intermediate Li[H_2Bpin] being +13 kcal mol^{-1} (Fig. S96†).

Despite its thermodynamic feasibility, this mechanism fails to explain the experimentally observed formation of [BH_4]$^-$ and B_2pin_3. To take these two species into account, we further investigated their formation from decomposition of [H_2Bpin]$^-$.

We first calculated the complete reduction of 1 equiv. HBpin by 3 equiv. Li_2[**4**]. The energetically costly formation of 1 equiv. Li_2[pin] per equivalent of Li[BH_4] generated renders this reaction exceedingly endergonic and thermodynamically out of scope (+36 kcal mol^{-1}, Fig. S95†; H_2pin = pinacol).

As an alternative approach, we propose a stepwise decomposition of Li[H_2Bpin] *via* B–H/B–O σ-bond metathesis with 2 equiv. HBpin (Fig. S97†). Formation of the final products Li[BH_4] and B_2pin_3 is exergonic by −21 kcal mol^{-1}, likely due to the isodesmic nature of this reaction and to the formation of two stable BO_3 motifs. Once formed, Li[BH_4] takes on the role as the actual imine-reducing agent. On this basis, we can now establish a catalytic cycle for hydroboration of Ph(H)C═N*t*Bu by HBpin that is fully consistent with all our experimental results (Fig. 4): in a first step, transition metal-like addition of HBpin to precatalyst Li_2[**2**] affords Li_2[**4**], the starting point of catalytic Cycle I (Fig. 4a, right). While the newly formed B–B bond persists throughout all subsequent reaction steps, the H^- ligand on Li_2[**4**] is transferred to a second HBpin molecule from solution. The free energy of the intermediates Li[**5**] and Li[H_2Bpin] amounts to +19 kcal mol^{-1} when referenced to the starting point of the cycle, Li_2[**4**] (Fig. 4b, right). This energy penalty, which is equivalent to the most endergonic step of the reaction sequence, results from the loss of π conjugation in the H^- carrier Li[H_2Bpin]. As outlined above, decomposition of Li[H_2Bpin] generates Li[BH_4]. In a slightly exergonic reaction,

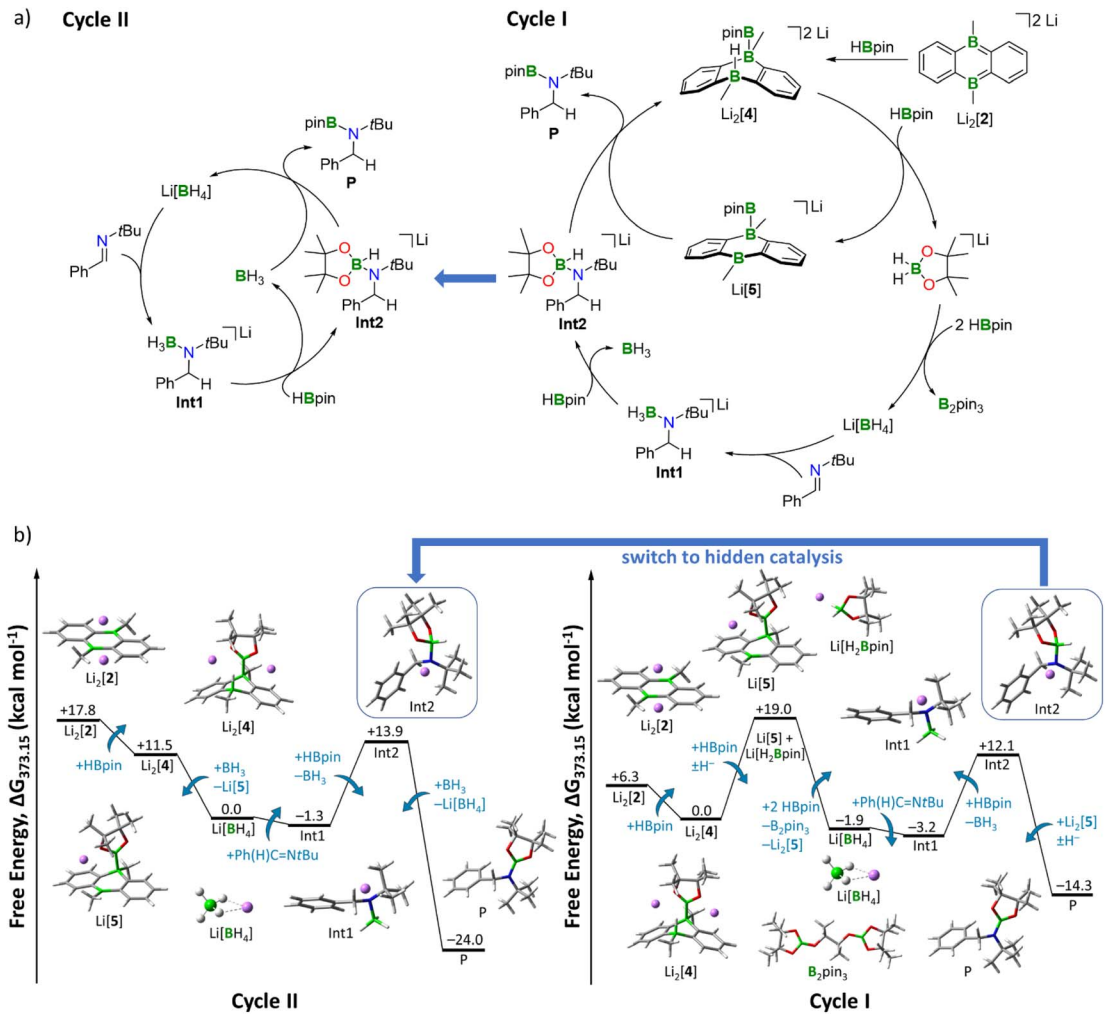

Fig. 4 (a) (Right) Catalytic Cycle I (hydride shuttle: Li[H_2Bpin]). (Left) Catalytic Cycle II, hidden catalysis (hydride shuttle: Li[BH_4]). (b) (Right) Free energy diagram for catalytic Cycle I. (Left) Free energy diagram for hidden catalysis Cycle II including BH_3·thf/Li[BH_4]. Energies are referenced to the starting point of the respective cycle. Level of theory: SMD(solvent = THF)/ωB97XD/6-311++G(d,p) from optimized structures at SMD(solvent = THF)/ωB97XD/6-31+G(d,p). Explicit thf molecules are omitted for clarity.

the double bond of Ph(H)C=N*t*Bu inserts into a B–H bond of $[BH_4]^-$, affording the amide-borane adduct **Int1**. The next step involves a ligand exchange at the negatively charged N atom of **Int1** through nucleophilic attack of **Int1** on HBpin from solution, which releases $BH_3\cdot$thf and forms **Int2**.[52] **Int2** possesses an activated H–Bpin bond (compare again Clark's intermediate) and thus represents the second highest thermodynamic barrier (+12 kcal mol^{-1}) of Cycle I (Fig. 4b, right). For the last reaction step, there are two possible options, which leads to a bifurcation of the catalytic cycle into Cycles I and II (Fig. 4a). Following Cycle I, Li[**5**] abstracts the H^- ligand from **Int2** in a notably exergonic reaction (−26 kcal mol^{-1}). As a result, the hydroboration product **P** is formed and Cycle I can start anew. The second possibility to produce **P** is H^- transfer from **Int2** to $BH_3\cdot$thf (generated in the preceding step), thereby entering Cycle II (left panels of Fig. 4a and b). The driving force to **P** is significantly higher along Cycle II (−38 kcal mol^{-1}) than along Cycle I (−26 kcal mol^{-1}). Moreover, since Cycle II starts from Li[BH_4] rather than Li_2[**4**], it bypasses the formation of Li[**5**] and Li[H_2Bpin], the highest-lying intermediate of Cycle I. The steps between the formation of Li[BH_4] and the formation of **Int2** are equivalent in both cycles. Given that $BH_3\cdot$thf has the highest H^- affinity of all species along Cycles I and II (Table S8†), it will take over the role as H^- shuttle as soon as it is available, effectively making the DBAs Li_2[**4**] and Li[**5**] obsolete. We, therefore, predict that only in the beginning the reaction proceeds with activation of HBpin by Li_2[**2**]. After a few cycles, the mechanism switches to hidden catalysis, where $BH_3\cdot$thf is the catalytically active species. From this point on, Cycle II outcompetes Cycle I.

Computational characterization of hydroboration Mechanism II. As previously discussed, less sterically demanding substrates than Ph(H)C=N*t*Bu readily form bicyclo[2.2.2]octadiene derivatives by [4 + 2] cycloaddition to Li_2[**2**] at room temperature. For the following reasons, the combination of Ph(H)C=NPh and Li_2[**14**] was chosen as representative model system for our theoretical study: (i) Li_2[**14**] should be the most challenging candidate to evaluate the feasibility of the key ring-opening step in our proposed catalytic mechanism, because, unlike bridging O or NR units, CH_2 fragments do not carry electron lone pairs as obvious sites of attack for incoming HBpin molecules (see Scheme 5). (ii) Li_2[**14**] possesses a symmetric scaffold so that only one kind of reactive center has to be considered.

Our proposed catalytic cycle for the Li_2[**14**]-mediated hydroboration of Ph(H)C=NPh is shown in Fig. 5; the corresponding free energies of the intermediates/transition states along the reaction path are depicted in Fig. 6. Similar to Mechanism I, the first step of Mechanism II is again activation of HBpin, but the actual mode is different: instead of the previously observed transition metal-like cleavage of the H–Bpin bond, the borane is now nucleophilically attacked by a bridging CH_2 group of Li_2[**14**].[53]

As a consequence, the tricyclic scaffold is opened, leading to formation of a tetracoordinate C–(H)Bpin unit and a tricoordinate DBA-B center (**Int3**; Fig. 6). **Int3** lies about +7 kcal mol^{-1} above the reactants. The corresponding barrier (**TS1**) amounts to about +25 kcal mol^{-1}. The activated H^- ligand of the C–(H)Bpin moiety in **Int3** is subject to intramolecular H^- transfer to the tricoordinate DBA-B center. This H^- shift restores the π-conjugated BO_2 motif in the Bpin residue and an electron octet on the DBA-B atom to afford the stabilized intermediate **Int4**, which lies only about +1 kcal mol^{-1} above the reactants. The corresponding barrier (**TS2**) is about +15 kcal mol^{-1} higher in energy than the reactants, *i.e.* considerably lower than the barrier of the first step. **Int4** then acts as an H^- donor to the imine, generating the amide $[Ph(H_2)C–NPh]^-$. The barrier of this step is about +3 kcal mol^{-1} and the resulting **Int5** is −18 kcal mol^{-1} lower in energy than the reactants.[54] $[Ph(H_2)C–NPh]^-$ forms an adduct with the Bpin residue of **Int5**, affording **Int6** (−13 kcal mol^{-1}). The corresponding barrier lies −1 kcal mol^{-1} below the reactants and +17 kcal mol^{-1} above **Int5**. The latter barrier height would have to be overcome if the reaction energy of the **Int4** → **Int5** step is instantaneously dissipated into the solvent. If this is not the case, the barrier associated with **TS4** would in fact be lower. In any case, the barrier of the **Int5** → **Int6** step is at least 8 kcal mol^{-1} lower than the rate-determining **TS1** (+25 kcal mol^{-1}). The catalytic cycle is completed by the restitution of the tricyclic framework of $[\mathbf{14}]^{2-}$ and the simultaneous release of the hydroboration product $Ph(H)_2C–N(Bpin)Ph$ (**P′**). The barrier of this last step is about +3 kcal mol^{-1} above the reactants (+16 kcal mol^{-1} above the previous intermediate) while the exothermicity of the overall reaction is high (−29 kcal mol^{-1}).

As a final remark on key technical details of the calculations, we emphasize that the first step of the mechanism, *i.e.*, nucleophilic attack of the C_2 bridge on HBpin, possesses by far the highest barrier (**TS1**; Fig. 6). It is about +10 kcal mol^{-1} higher

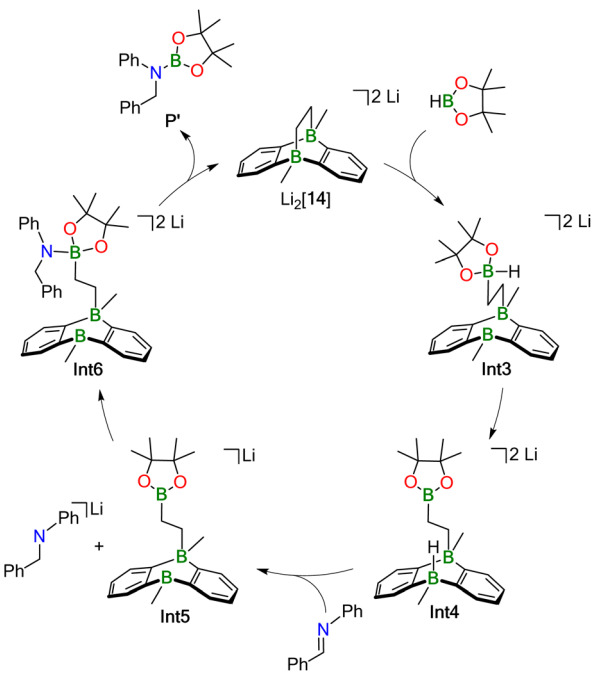

Fig. 5 Hydroboration Mechanism II for less sterically demanding substrates. The corresponding energy diagram is given in Fig. 6.

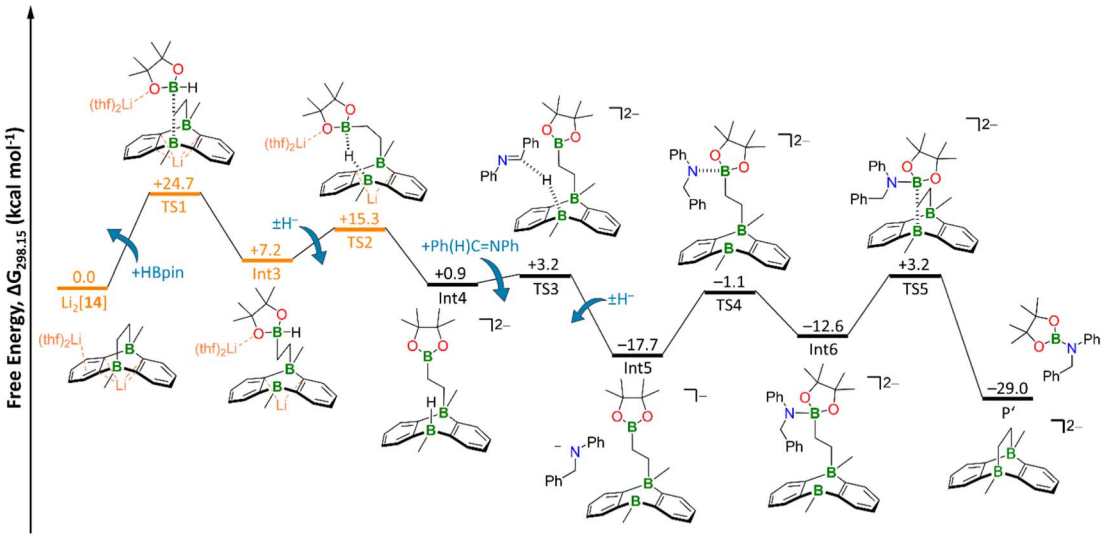

Fig. 6 Free energy diagram of hydroboration Mechanism II. Orange: transition states and intermediate including counterions and explicit solvent molecules. The **TS2** geometry was obtained *via* a relaxed scan (Fig. S100†) and subsequent restricted optimization of the counterions and explicit THF molecules. **TS3** and **TS4** geometries were obtained *via* relaxed scans (Fig. S101 and S102,† respectively). Level of theory: SMD(solvent = THF)/ωB97XD/6-311++G(d,p) from optimized structures at SMD(solvent = THF)/ωB97XD/6-31+G(d,p).

than the second highest barrier (**TS2**) with respect to the reactants. Concerning the respective preceding intermediate, the difference is even larger (+25 kcal mol^{-1} *vs.* +8 kcal mol^{-1}) since **Int3** lies about +7 kcal mol^{-1} above the reactants.

Hence, we investigated the influence of the counterions and their first solvation shell on the performance of the catalyst for both steps in more detail. Rather than modeling the effects of the Li^+ counter cations and explicit THF solvent molecules, we tested the consequences of a mere inclusion of continuum effects by the SMD model. We found the resulting barrier for the trigonal-bipyramidal transition state (**TS1**) to increase by +7 kcal mol^{-1} to +32 kcal mol^{-1}, which is too high considering the experimental conditions. Furthermore, **TS2** is also destabilized by +4 kcal mol^{-1} (Fig. S98†). This effect can be rationalized by considering coordination of the Li^+ cation *via* the O atom of the HBpin molecule. Electron density is thereby withdrawn from the adjacent B center, rendering it more electrophilic and, in turn, facilitating its attack on the electron-rich C_2 bridge of Li_2[**14**]. Furthermore, the tetracoordinate B center in the resulting **Int3** is also stabilized by a $Li^+\cdots O$ interaction (Fig. S98†). Since all other barriers are significantly lower than **TS1** and **TS2**, we calculated them – as well as the corresponding intermediates – without explicit counterions and THF molecules to reduce calculation cost.

Conclusions

We have successfully expanded the range of $[DBA\text{-}Me_2]^{2-}$-catalyzed reactions to include hydroborations with pinacolborane (HBpin; DBA-Me_2 = 9,10-dimethyl-9,10-dihydro-9,10-diboraanthracene). In comparison to analogous hydrogenation reactions, distinct differences become apparent: the general entry step for $[DBA\text{-}Me_2]^{2-}$-catalyzed hydrogenations is H–H-bond addition across the two B atoms of the doubly reduced arylborane. Thus, any competing [4 + 2] cycloaddition reaction between the unsaturated substrate (to be hydrogenated) and the $[DBA\text{-}Me_2]^{2-}$ dianion leads to catalyst poisoning. Although H–Bpin-bond activation with $[DBA\text{-}Me_2]^{2-}$ is also possible, it only plays a role in the hydroboration of sterically loaded substrates such as Ph(H)C=N*t*Bu and proceeds *via* HBpin degradation to $[BH_4]^-$ and B_2pin_3, providing an example of "hidden borohydride catalysis". In all other cases where [4 + 2] cycloaddition to $[DBA\text{-}Me_2]^{2-}$ is not hampered by the steric demands of the substrates (*e.g.*, Ph(H)C=NPh), the cycloadducts are not dead ends, but rather constitute the active hydroboration catalysts. Using the hydroboration of Ph(H)C=NPh with HBpin, mediated by the cycloadduct between $[DBA\text{-}Me_2]^{2-}$ and $H_2C{=}CH_2$, as representative model reaction, we have unveiled the underlying reaction mechanism in a joint experimental and theoretical effort: the 1,2-ethanediyl-bridged tricyclic catalyst can be viewed as intramolecular B–C adduct, in which a Lewis-acidic tricoordinate DBA-B center protects a Lewis-basic $[{:}CH_2{-}CH_2{-}B(Me)Ar_2]^{2-}$ fragment to create a stable resting state. In the presence of HBpin, the tricycle can reversibly open to form an HBpin-alkyl adduct in which the H–Bpin bond is activated for H^- transfer to the tricoordinate DBA-B center, from which H^- migrates further to the polar Ph(H)C=NPh bond. The resulting amide $[Ph(H)_2C{-}NPh]^-$ takes up $[Bpin]^+$ from $[pinB{-}CH_2{-}CH_2{-}B(Me)Ar_2]^-$ to form $Ph(H)_2C{-}N(Bpin)Ph$, thereby regenerating the catalyst and completing the catalytic cycle. According to thorough DFT calculations, our mechanistic proposal is energetically feasible under the experimentally applied reaction conditions (room temperature, THF-d_8, Li^+ counter cations). Quantum-chemical calculations by Kinjo and coworkers have led them to explicitly rule out such a scenario for their related neutral bicyclo[2.2.2]octadienes, assembled from 1,3,2,5-diazadiborinines rather than $[DBA\text{-}Me_2]^{2-}$ dianions.[7] Instead, they postulated

H–Bpin-bond activation through electrostatic interactions with positively polarized regions of the still intact tricyclic catalyst. This comparison clearly demonstrates the multifaceted character of doubly B-doped bicyclo[2.2.2]octadienes and shows how seemingly subtle modifications of their molecular scaffolds can significantly alter their catalytic properties. In the future, it will be interesting to explore what else this class of compounds can contribute to the field of main group catalysis.

Data availability

The datasets supporting this article have been uploaded as part of the ESI.†

Author contributions

S. E. P. performed all preparative experiments. C. H. performed all calculations. M. B. performed the X-ray crystal structure analyses. F. F., H.-W. L, B. E., and M. W. supervised the project. The manuscript was written through contributions of all authors.

Conflicts of interest

There are no conflicts to declare.

Notes and references

1 G. Erker and D. W. Stephan, *Frustrated Lewis Pairs I & II*, Springer, Heidelberg, 2013.
2 A. R. Jupp and D. W. Stephan, *Trends Chem.*, 2019, **1**, 35–48.
3 S. E. Prey and M. Wagner, *Adv. Synth. Catal.*, 2021, **363**, 2290–2309.
4 Y. Su and R. Kinjo, *Chem. Soc. Rev.*, 2019, **48**, 3613–3659.
5 D. Wu, L. Kong, Y. Li, R. Ganguly and R. Kinjo, *Nat. Commun.*, 2015, **6**, 7340.
6 D. Wu, R. Ganguly, Y. Li, S. N. Hoo, H. Hirao and R. Kinjo, *Chem. Sci.*, 2015, **6**, 7150–7155.
7 D. Wu, R. Wang, Y. Li, R. Ganguly, H. Hirao and R. Kinjo, *Chem*, 2017, **3**, 134–151.
8 B. Wang, Y. Li, R. Ganguly, H. Hirao and R. Kinjo, *Nat. Commun.*, 2016, **7**, 11871.
9 B. Wang and R. Kinjo, *Tetrahedron*, 2018, **74**, 7273–7276.
10 A. Lorbach, M. Bolte, H.-W. Lerner and M. Wagner, *Organometallics*, 2010, **29**, 5762–5765.
11 E. von Grotthuss, M. Diefenbach, M. Bolte, H.-W. Lerner, M. C. Holthausen and M. Wagner, *Angew. Chem., Int. Ed.*, 2016, **55**, 14067–14071.
12 E. von Grotthuss, S. E. Prey, M. Bolte, H.-W. Lerner and M. Wagner, *Angew. Chem., Int. Ed.*, 2018, **57**, 16491–16495.
13 E. von Grotthuss, S. E. Prey, M. Bolte, H.-W. Lerner and M. Wagner, *J. Am. Chem. Soc.*, 2019, **141**, 6082–6091.
14 E. von Grotthuss, F. Nawa, M. Bolte, H.-W. Lerner and M. Wagner, *Tetrahedron*, 2019, **75**, 26–30.
15 Harman *et al.* have reported a number of remarkable (catalytic) transformations mediated by Au complexes of bidentate diphosphine ligands with DBA backbones: (*a*) J. W. Taylor, A. McSkimming, M.-E. Moret and W. H. Harman, *Angew. Chem., Int. Ed.*, 2017, **56**, 10413–10417; (*b*) J. W. Taylor, A. McSkimming, L. A. Essex and W. H. Harman, *Chem. Sci.*, 2019, **10**, 9084–9090; (*c*) J. W. Taylor and W. H. Harman, *Chem. Commun.*, 2020, **56**, 4480–4483; (*d*) J. W. Taylor and W. H. Harman, *Chem. Commun.*, 2020, **56**, 13804–13807.
16 (*a*) M. A. Dureen, A. Lough, T. M. Gilbert and D. W. Stephan, *Chem. Commun.*, 2008, 4303–4305; (*b*) P. Eisenberger, A. M. Bailey and C. M. Crudden, *J. Am. Chem. Soc.*, 2012, **134**, 17384–17387; (*c*) D. W. Stephan, *Acc. Chem. Res.*, 2015, **48**, 306–316; (*d*) F.-G. Fontaine, M.-A. Courtemanche, M.-A. Légaré and É. Rochette, *Coord. Chem. Rev.*, 2017, **334**, 124–135; (*e*) P. Vasko, I. A. Zulkifly, M. Á. Fuentes, Z. Mo, J. Hicks, P. C. J. Kamer and S. Aldridge, *Chem.–Eur. J.*, 2018, **24**, 10531–10540; (*f*) A. Falconnet, M. Magre, B. Maity, L. Cavallo and M. Rueping, *Angew. Chem., Int. Ed.*, 2019, **58**, 17567–17571; (*g*) Y. Lebedev, I. Polishchuk, B. Maity, M. Dinis Veloso Guerreiro, L. Cavallo and M. Rueping, *J. Am. Chem. Soc.*, 2019, **141**, 19415–19423; (*h*) D. W. Stephan, *Chem*, 2020, **6**, 1520–1526.
17 A. D. Bage, K. Nicholson, T. A. Hunt, T. Langer and S. P. Thomas, *ACS Catal.*, 2020, **10**, 13479–13486.
18 K. Wade, *Electron Deficient Compounds*, Springer, New York, 1971.
19 I. A. I. Mkhalid, J. H. Barnard, T. B. Marder, J. M. Murphy and J. F. Hartwig, *Chem. Rev.*, 2010, **110**, 890–931.
20 See the ESI† for further details.
21 The free Gibbs energy for the reaction $[Li(thf)_2]_2$[**4**] + THF → $[Li(thf)_2]$[**5**] + $[Li(thf)_3]H$ amounts to +27.4 kcal mol^{-1} at room temperature.
22 W. Clegg, A. J. Scott, C. Dai, G. Lesley, T. B. Marder, N. C. Norman and L. J. Farrugia, *Acta Crystallogr., Sect. C: Cryst. Struct. Commun.*, 1996, **52**, 2545–2547.
23 The ^{11}B NMR signal of the Bpin group in Na_2[**4**] (42.6 ppm; THF-d_8) may seem unusually downfield shifted, as the resonance of B_2pin_2 appears at 32.6 ppm (own measurement in THF-d_8). However, the signals of Bpin groups attached to anionic, tetracoordinate B centers appear in the same range as that of Na_2[**4**] (*cf.* K[B_2pin_2·OtBu] δ = 41.1; THF-d_8): S. Pietsch, E. C. Neeve, D. C. Apperley, R. Bertermann, F. Mo, D. Qiu, M. S. Cheung, L. Dang, J. Wang, U. Radius, Z. Lin, C. Kleeberg and T. B. Marder, *Chem.–Eur. J.*, 2015, **21**, 7082–7099. The calculated ^{11}B NMR shifts of $[Na(thf)_2]_2$[**4**] are: δ = 45.8 (Bpin), −18.9 (BH), −23.3 (*B*Bpin) (GIAO method at the SMD(solvent = THF)/ωB97XD/6-311++G(d,p) level).
24 Further B–Bpin bond lengths (Å) useful for comparison are (a) B_2pin_2 = 1.7041(15), (b) [K(18-c-6)][B_2pin_2OMe] = 1.753(2); [Me_4N][B_2pin_2F]·THF = 1.736(8), and (c) [Mg(HC-{(Me)CN(2,6-*i*$Pr_2C_6H_3$)}$_2$)][pinB–BPh_3] = 1.718(7): (*a*) C. Kleeberg, A. G. Crawford, A. S. Batsanov, P. Hodgkinson, D. C. Apperley, M. S. Cheung, Z. Lin and T. B. Marder, *J. Org. Chem.*, 2012, **77**, 785–789; (*b*) ref. 23; (*c*) A.-F. Pécharman, M. S. Hill, C. L. McMullin and M. F. Mahon, *Angew. Chem., Int. Ed.*, 2017, **56**, 16363–16366.

25 E. C. Neeve, S. J. Geier, I. A. I. Mkhalid, S. A. Westcott and T. B. Marder, *Chem. Rev.*, 2016, **116**, 9091–9161.
26 A. B. Cuenca, R. Shishido, H. Ito and E. Fernández, *Chem. Soc. Rev.*, 2017, **46**, 415–430.
27 C. Kleeberg and C. Borner, *Eur. J. Inorg. Chem.*, 2013, **2013**, 2799–2806.
28 Li[$SiPh_3$] was chosen as the nucleophile, because its high steric demand disfavors the formation of a stable adduct with the tricoordinate DBA-B atom in Li[**5**]. Moreover, silylboranes such as Ph_3Si–Bpin have considerable application potential: (*a*) T. Ohmura and M. Suginome, *Bull. Chem. Soc. Jpn.*, 2009, **82**, 29–49; (*b*) M. Oestreich, E. Hartmann and M. Mewald, *Chem. Rev.*, 2013, **113**, 402–441; (*c*) S. Bähr, W. Xue and M. Oestreich, *ACS Catal.*, 2019, **9**, 16–24; (*d*) C. Moberg, *Synthesis*, 2020, **52**, 3129–3139; (*e*) K. Hirano and M. Uchiyama, *Adv. Synth. Catal.*, 2021, **363**, 2340–2353; (*f*) J.-J. Feng, W. Mao, L. Zhang and M. Oestreich, *Chem. Soc. Rev.*, 2021, **50**, 2010–2073.
29 G. Becker, H.-M. Hartmann, A. Münch and H. Riffel, *Z. Anorg. Allg. Chemie*, 1985, **530**, 29–42.
30 Quantitative deprotonation of Li[**6**] is also possible using $Ph(H)_2C$–N(Li)*t*Bu as the base. Given that the amide can be formed through H^- transfer to Ph(H)C=N*t*Bu, this deprotonation experiment also marks the hitherto missing keystone of the reaction mechanism previously proposed for the catalytic hydrogenation of the imine by Li_2[**2**]/H_2: In contrast to conventional FLPs, the H_2-activation product Li_2[**11**] (Scheme 3) delivers first an H^- and second an H^+ ion (*cf.* ref. 13).
31 T. Wassmann, A. P. Seitsonen, A. M. Saitta, M. Lazzeri and F. Mauri, *J. Am. Chem. Soc.*, 2010, **132**, 3440–3451.
32 For the following reasons, Li_2[**2**] was chosen despite its somewhat different behavior toward HBpin compared to the other M_2[**1**]/M_2[**2**] compounds: (i) the neutral Me-substituted DBA **2** is more convenient to handle than its H-substituted congener **1**. (ii) We have already published the Li^+ salts of some cycloadducts between $[DBA\text{-}Me_2]^{2-}$ and unsaturated substrates, which are the actual catalytically active species and thus the focus of our mechanistic investigations (*cf.* ref. 12 and 13). (iii) Since our DFT calculations include the counter cations, the computational cost for the treatment of Li^+ is lower than for the treatment of Na^+/K^+.
33 We initially relied on this protocol because it is most similar to the one applied for our earlier hydrogenation reactions (*cf.* ref. 13), which we want to use for comparison. Later, it was found that adding the unsaturated substrate first is essential to exclude contributions of the hidden borohydride catalysis as an undesired background reaction.
34 X. Wang and X. Xu, *RSC Adv.*, 2021, **11**, 1128–1133.
35 A. R. Gatti and T. Wartik, *Inorg. Chem.*, 1966, **5**, 329–330.
36 M. Magre, M. Szewczyk and M. Rueping, *Chem. Rev.*, 2022, **122**, 8261–8312.
37 Sen *et al.* identified a comparable $Li^+\cdots O$ coordination as the key interaction in lithium phenolate-catalyzed HBpin additions to carbonyl compounds. The resulting decrease in O=B π donation leads to an increase in the Lewis acidity of the HBpin molecule and in turn facilitates its interaction with the carbonyl-O atom. We adopted such a scenario to Li_2[**14**] and computed a corresponding reaction barrier of +31 kcal mol^{-1}. Although this value is lower than that of the uncatalyzed reaction by –14 kcal mol^{-1}, it is still higher than **TS1** by +6 kcal mol^{-1}. Since **TS1** represents the highest barrier in our hydroboration Mechanism II (see the ESI† for details), also Sen's mechanism can be ruled out for our case: M. K. Bisai, T. Das, K. Vanka and S. S. Sen, *Chem. Commun.*, 2018, **54**, 6843–6846.
38 Hydroboration of Ph(H)C=NPh with HBpin in THF-d_8 required about the same time, regardless of whether Li_2[**14**] or Na_2[**14**] was used as the catalyst (NMR-spectroscopic control). We take this as justification that Li_2[**14**] is a representative example catalyst to study Mechanism II. It should also be noted that the necessary explicit treatment of the counter cation's coordination sphere is much more complex in the case of the larger Na^+. Its coordination sphere includes six neighbors while the one of Li^+ only contains four. Consequently, not only does the size of the system increase, but also a greater variety of coordination polyhedra can be expected.
39 C. Weetman, M. S. Hill and M. F. Mahon, *Chem.–Eur. J.*, 2016, **22**, 7158–7162.
40 D. Mukherjee, S. Shirase, T. P. Spaniol, K. Mashima and J. Okuda, *Chem. Commun.*, 2016, **52**, 13155–13158.
41 M. D. Anker, M. Arrowsmith, R. L. Arrowsmith, M. S. Hill and M. F. Mahon, *Inorg. Chem.*, 2017, **56**, 5976–5983.
42 A. Ramos, A. Antiñolo, F. Carrillo-Hermosilla, R. Fernández-Galán and D. García-Vivó, *Chem. Commun.*, 2019, **55**, 3073–3076.
43 N. Sarkar, S. Bera and S. Nembenna, *J. Org. Chem.*, 2020, **85**, 4999–5009.
44 J.-D. Chai and M. Head-Gordon, *Phys. Chem. Chem. Phys.*, 2008, **10**, 6615–6620.
45 R. Krishnan, J. S. Binkley, R. Seeger and J. A. Pople, *J. Chem. Phys.*, 1980, **72**, 650–654.
46 T. Clark, J. Chandrasekhar, G. W. Spitznagel and P. von Ragué Schleyer, *J. Comput. Chem.*, 1983, **4**, 294–301.
47 A. V. Marenich, C. J. Cramer and D. G. Truhlar, *J. Phys. Chem. B*, 2009, **113**, 6378–6396.
48 A. Ben-Naim, *J. Phys. Chem.*, 1978, **82**, 792–803.
49 J. R. Pliego Jr and J. M. Riveros, *Phys. Chem. Chem. Phys.*, 2002, **4**, 1622–1627.
50 M. J. Frisch, G. W. Trucks, H. B. Schlegel, G. E. Scuseria, M. A. Robb, J. R. Cheeseman, G. Scalmani, V. Barone, G. A. Peterson, H. Nakatsuji, X. Li, M. Caricato, A. V. Marenich, J. Bloino, B. G. Janesko, R. Gomperts, B. Mennucci, H. P. Hratchian, J. V. Ortiz, A. F. Izmaylov, J. L. Sonnenberg, D. Williams-Young, F. Ding, F. Lipparini, F. Egidi, J. Goings, B. Peng, A. Petrone, T. Henderson, D. Ranasinghe, V. G. Zakrzewski, J. Gao, N. Rega, G. Zheng, W. Liang, M. Hada, M. Ehara, K. Toyota, R. Fukuda, J. Hasegawa, M. Ishida, T. Nakajima, Y. Honda, O. Kitao, H. Nakai, T. Vreven, K. Throssell, J. A. Montgomery Jr, J. E. Peralta, F. Ogliaro,

M. J. Bearpark, J. J. Heyd, E. N. Brothers, K. N. Kudin, V. N. Staroverov, T. A. Keith, R. Kobayashi, J. Normand, K. Raghavachari, A. P. Rendell, J. C. Burant, S. S. Iyengar, J. Tomasi, M. Cossi, J. M. Millam, M. Klene, C. Adamo, R. Cammi, J. W. Ochterski, R. L. Martin, K. Morokuma, O. Farkas, J. B. Foresman and D. J. Fox, *Gaussian 16 (Revision A.03)*, Gaussian Inc., Wallingfort, CT, USA, 2016.

51 I. P. Query, P. A. Squier, E. M. Larson, N. A. Isley and T. B. Clark, *J. Org. Chem.*, 2011, **76**, 6452–6456.

52 Another possible source of Bpin residues is Li[**5**]. Attack of **Int1** at the Bpin substituent of Li[**5**] would lead to the immediate formation of **P** and Li_2[**2**] *via* [Bpin]$^+$ transfer and with release of BH_3·thf (*cf.* the analogous reaction Li[$SiPh_3$] + Li[**5**] → pinB–$SiPh_3$ + Li_2[**2**]; Scheme 2). According to our calculations this alternative scenario would lead to a decrease in the driving force of the overall reaction from −14 kcal mol^{-1} to −8 kcal mol^{-1}. On the other hand, formation of **Int2** (+15 kcal mol^{-1}) would be bypassed. However, an interaction between the amide anion of **Int1** and negatively charged [**5**]$^-$ is electrostatically unfavorable and the reactive B(pin) center of [**5**]$^-$ is sterically less accessible than that of HBpin. We therefore assume that the thermodynamically less favorable formation of **Int2** (+15 kcal mol^{-1}) is preferred by kinetics. Since the formation of Li[**5**] and Li[H_2Bpin], which is the energetically most costly step of Cycle I, is not circumvented, a switch to Cycle II will take place in any case.

53 An analogous attack of a B-bonded Me residue on HBpin or a B–H/B–C σ-bond metathesis leading directly to **Int4** (Fig. 5) can be ruled out due to significantly higher reaction barriers (Fig. S98,† **TSa** and **TSb**).

54 H$^-$ transfer to the alternative electrophile HBpin would be thermodynamically less favorable by +13 kcal mol^{-1}. In general, HBpin appears to be the weakest H$^-$ acceptor of the investigated species (see Table S8†).